Scientific Research Publishing

Journal of Materials Science and Chemical Engineering, 2023, 11, 127-134
https://www.scirp.org/journal/msce
ISSN Online: 2327-6053
ISSN Print: 2327-6045

Active Truss Metamaterials: Modelling and Tuning of Band Gaps

Daniel Calegaro, Stefano Mariani

Department of Civil and Environmental Engineering, Politecnico di Milano, Milano, Italy
Email: stefano.mariani@polimi.it

How to cite this paper: Calegaro, D. and Mariani, S. (2023) Active Truss Metamaterials: Modelling and Tuning of Band Gaps. *Journal of Materials Science and Chemical Engineering*, **11**, 127-134.
https://doi.org/10.4236/msce.2023.118008

Received: August 6, 2023
Accepted: August 28, 2023
Published: August 31, 2023

Abstract

Periodic composite structures, like acoustic metamaterials (AMMs) and phononic crystals (PCs), are able to prevent the propagation of sound and elastic waves for some specific frequency ranges, leading to the emergence of so-called band gaps. So far, the optimization of the metamaterial properties and therefore of the band gaps has been typically performed on passive PCs and AMMs. Hence, the band gap properties cannot be tuned anymore after the production process of the metamaterials; this problem can be overcome thanks to the use of active materials. In this work, material and geometric nonlinearities are exploited to actively tune the frequency ranges of the band gaps of an architected AMM characterized by a three-dimensional periodicity. Specifically, a hyperelastic piezoelectric composite, that can be obtained by embedding piezo nanoparticles in a soft polymeric matrix, is considered to assess the effects of the nonlinearities on the behavior of sculptured microstructures, taking advantage of instability-induced pattern transformation and piezoelectricity to actively tune the band gaps.

Keywords

Acoustic Metamaterials, Hyperelasticity, Multi-Physics, Piezoelectricity, Buckling

1. Introduction

A metamaterial is usually considered to be engineered in order to display properties not found in nature. Even though such a definition can be controversial, they can surely be used to make things like light and sound "*dance to our tune*" [1]. Acoustic metamaterials (AMMs) and phononic crystals (PCs) are two different classes of periodic composites able to tailor the path of sound and elastic waves travelling inside them, to let band gaps emerge so that frequency ranges

exist to (even selectively) prevent the propagation of the said waves. Such fundamental properties make metamaterials of interest for different applications, including vibration reduction devices for vehicles and structures, waveguides and acoustic cloaking [2].

So far, most of the research activities related to band gap optimization have been conducted on passive PCs and AMMs [2]. In such cases, the geometrical and material properties are assumed constant after the production process, thereby limiting the possible applications requiring a real-time tuning of the working conditions. For these reasons, new strategies are sought to obtain active metamaterials with adaptive properties, and so adaptive band gaps. Recent works exploited the use of buckling instabilities to switch the pattern of wave propagations, transforming the phononic band gaps [2] [3] [4], and the adoption of AMMs with various modulation techniques driven by piezoelectric effect [5] [6] [7], temperature [8], and electric and magnetic biasing [9] [10].

In the present work, the tunability of band gaps arises from the combination of hyperelasticity and piezoelectricity. In this way, both material and geometric nonlinearities can be exploited to tune the dispersion of waves travelling into metamaterial cells obtained by assembling trusses in an architected local microstructure. In order to obtain a similar backbone material, piezoelectric (nano)particles can be embedded into a hyperelastic polymeric matrix. An example of these piezoelectric nanocomposite metamaterials was analyzed in [11]: during an experimental campaign under uniaxial compression, the metamaterial was severely deformed and its electrical properties were reported to change with the applied strain. However, a study of the vibration attenuation properties of such metamaterial was not been carried out in the original paper, and in the literature there is still a lack of investigations regarding this specific topic.

In this work, the focus is thus on the tunability of the band gaps of a hyperelastic piezoelectric AMM characterized by a three-dimensional periodicity of a representative volume featuring an architected arrangement of trusses or slender beams, taking advantage of instability-induced pattern transformation. The remainder of the paper is accordingly arranged as follows. In Section 2, a brief account of the continuum thermodynamics-based model for the studied AMM is provided. Section 3 is next devoted to the discussion of some preliminary results; due to length constraint, all the results of the current (numerical) investigation will be discussed in future developments of what presented here. Finally, some concluding remarks and proposals for future developments are gathered in Section 4.

2. Governing Equations

In (linear) theory of piezoelectricity, the electric enthalpy density h per unit volume in the current configuration is assumed to be, see also [12]:

$$h = \frac{1}{2} C^{E}_{ijkl} S_{kl} S_{ij} - e_{iml} S_{ml} \nabla_i V - \frac{1}{2} \varepsilon_{ij} \nabla_j V \nabla_i V, \tag{1}$$

where: indices $i,j,k,l,m=1,2,3$ denote the components of the various tensors described hereafter in a three-dimensional orthonormal reference frame; S_{ij} is the strain tensor; C^{E}_{ijkl} is the elasticity tensor; ∇_i is the spatial gradient operator, featuring derivatives with respect to the spatial coordinates; V is the electric potential; e_{iml} is the piezoelectric coupling tensor; and ε_{ij} is the dielectric permittivity tensor.

In this work, the electric enthalpy density for a hyperelastic piezoelectric material at finite strain is obtained by moving from Equation (1) and by adopting a proper form of the (internal) mechanical energy density [13]. The proposed solution, still formulated in the reference configuration, reads:

$$H=\Psi^{ME}\left(C_{ij}\right)-e_{iml}E_{ml}\nabla_{0,i}V-\frac{1}{2}\varepsilon JC^{-1}_{ij}\nabla_{0,j}V\nabla_{0,i}V, \tag{2}$$

where: $\Psi^{ME}\left(C_{ij}\right)$ is the stored energy density of the hyperelastic material; C_{ij} is the right Cauchy-Green tensor; $\nabla_{0,i}$ is the material gradient operator; ε is the dielectric permittivity constant; and J is the determinant of the deformation gradient. To be more specific, the hyperelastic energy density is chosen for a (compressible) Neo-Hookean material, that is:

$$\Psi^{ME}=\frac{1}{2}\mu\left(tr\left(C_{ij}\right)-3\right)-\mu\ln J+\frac{1}{2}\lambda\left(\ln J\right)^2, \tag{3}$$

where λ and μ are the relevant Lamé constants.

The second Piola-Kirchhoff stress tensor T_{ij} and the electric displacement D_k can then be obtained via differentiation of the electric enthalpy density, according to:

$$\begin{aligned} T_{ij}&=2\frac{\partial H}{\partial C_{ij}}\\ D_k&=-\frac{\partial H}{\partial\nabla_{0,k}V}\end{aligned} \tag{4}$$

3. Results

The multi-physics constitutive model reported in Section 2 has been implemented in the finite element software COMSOL Multiphysics® [14]. The geometry of the representative volume, or unit cell is shown in **Figure 1** and is characterized by the following dimensions: $a=1.55$ cm, $b=9.96a$ and $c=7.5a$. Periodic boundary conditions in terms of displacements are applied on the opposite sides of the cell.

The electromechanical properties of the composite material, assumed to be made of piezoelectric particles embedded inside a hyperelastic matrix, are directly taken from [11]: the Lamé constants of the Neo-Hookean model are $\lambda=65792$ MPa and $\mu=257$ MPa; the non-vanishing components of the stress-charge coupling tensor are $e_{113}=e_{123}=0.0336$ C/m^2, $e_{311}=0.00310$ C/m^2, $e_{322}=0.00850$ C/m^2 and $e_{333}=0.0291$ C/m^2; finally, the dielectric permittivity constant is $\varepsilon=0.2576\times10^{-9}$ C^2/(Nm^2) and the mass density is $\rho=1050$ kg/m^3.

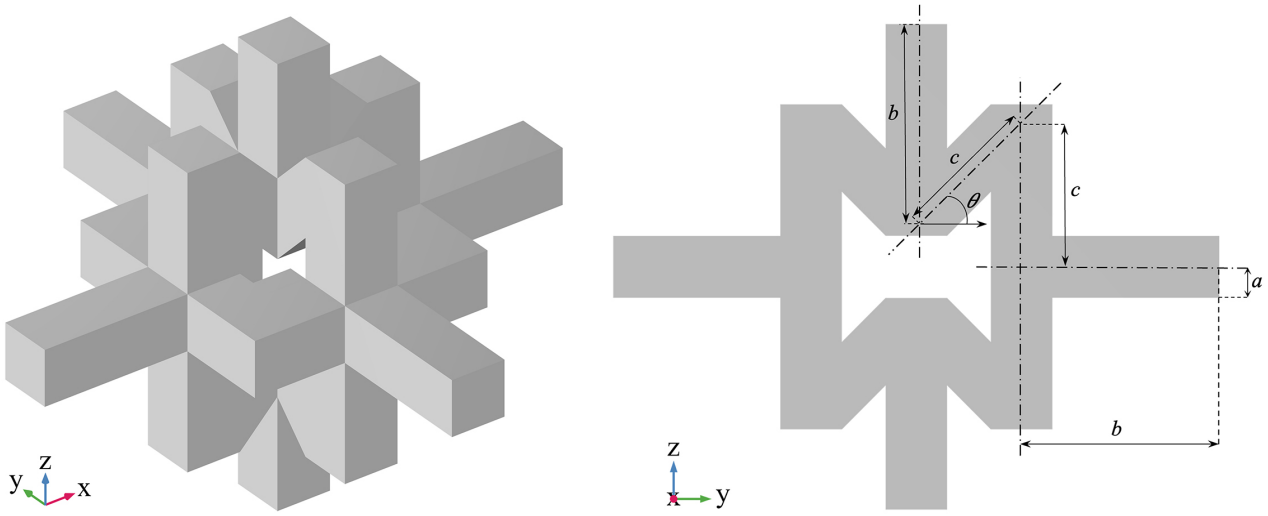

Figure 1. Modelled unit cell structure (left), and its cross-section with notation (right).

The considered architected periodic structure can show two main types of mechanical instabilities when loaded in compression: microscopic and macroscopic ones. The first type represents instabilities with wavelengths on the order of the microstructure size, while the second one displays larger wavelengths, comparable to the size of the whole unit cell [3]. In order to detect the onset of these instabilities and the corresponding pattern, the so-called Bloch-Floquet instability analysis has to be performed. The entire procedure consists of two steps. First, the unit cell undergoes static finite deformations through the application of general periodic boundary conditions. Second, the eigenfrequency problem is solved in the deformed configuration through the application of the Bloch periodic boundary conditions, by varying the wave vector in the direction of the applied load [7]. After the Bloch-Floquet instability analysis, a post buckling analysis is performed on the new, enlarged unit cell obtained on the basis of the pattern at microscopic instability. Finally, a set of eigenfrequency analyses is performed at different strain levels in the post-buckling regime, for specific wave paths.

In the analyses, a uniaxial compression is applied along the z direction, see **Figure 1**. The Bloch-Floquet instability analysis is performed at values of the angle θ to denote the inclination of the internal out-of-plane beams ranging between 0˚ and 45˚. The investigation has allowed to detect that the microscopic instability always occurs before the macroscopic one; the strain associated with the microscopic instability is reported in **Figure 2** at varying values of the aforementioned angle θ. This outcome testifies that the range and position of each band gap could change because of loading, due to the induced microstructural change; the other way around, if the instability exhibited a macroscopic behavior, the microstructure would not change during the deformation and so also the band gap properties. Hence, for what concerns the microscopic instability, the associated enlarged unit cell corresponds to $1 \times 2 \times 2$ primitive unit cells, independently on the θ value, see **Figure 2**.

The stress-strain plot resulting from the post-buckling analysis of the periodic structure is shown in **Figure 3** for $\theta = 45^{\circ}$. Four corresponding deformed configurations of the enlarged unit cell are reported in **Figure 4** for some characteristic values of the strain in the loading direction. Considering that the internal beams of length c inside each primitive unit cell can be referred to as "*mass*" due to their higher stiffness compared to the external beams of length b, also called "*elastic ligaments*" as they connect adjacent primitive unit cells, the following comments can be provided for the obtained results. The initial response, up to the critical strain incepting instability, is characterized by a uniform compression; then, the structure starts to bend according to the first buckling mode and a significant softening is observed, as testified by the change in the slope of the stress-strain diagram shown in **Figure 3**. In the post-buckling regime, most of the deformation affects the configuration of the ligaments, due to their lower rigidity, while the masses tend to rotate like rigid bodies.

The results of the eigenfrequency analysis are reported in **Figure 5** at different deformation levels (reported as positive even if in compression) and for different θ values. It can be seen that, as θ increases:

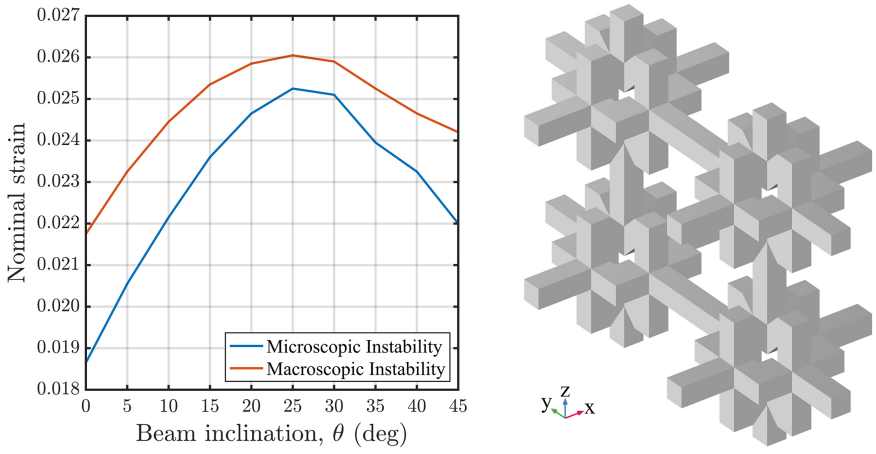

Figure 2. Effect of the beam slope θ on the strain levels at microscopic and macroscopic instabilities (left); enlarged unit cell corresponding to microscopic instability, reported for $\theta = 45^{\circ}$ (right).

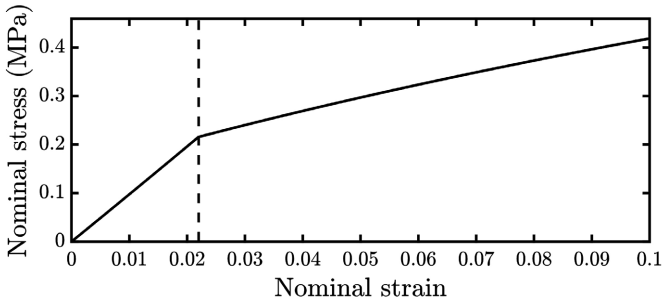

Figure 3. Stress-strain response of the enlarged unit cell characterized by $\theta = 45^{\circ}$ and loaded in the z direction. In the plot, the vertical dotted line corresponds to the inception of microscopic instability for $E_{33} = 0.022$.

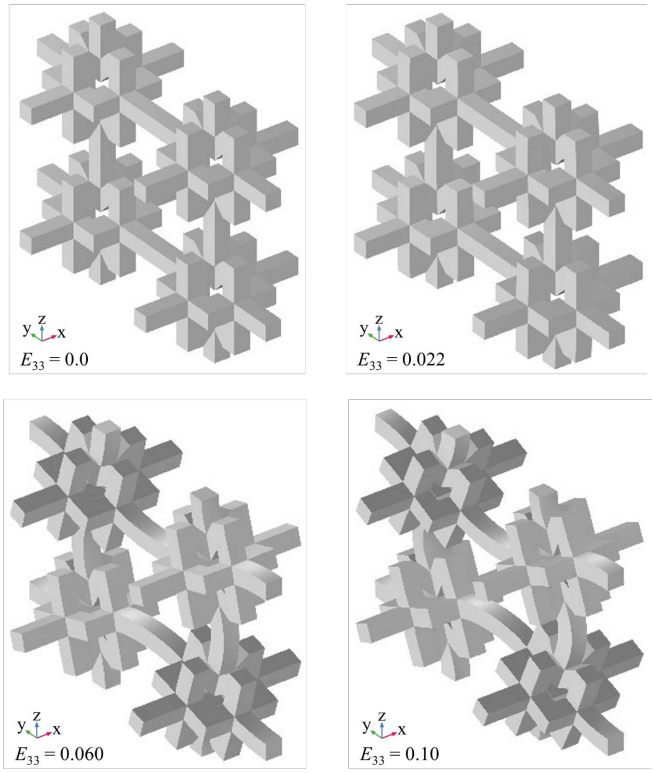

Figure 4. Deformed configurations of the architected unit cell characterized by $\theta = 45^{\circ}$ and loaded in the z direction.

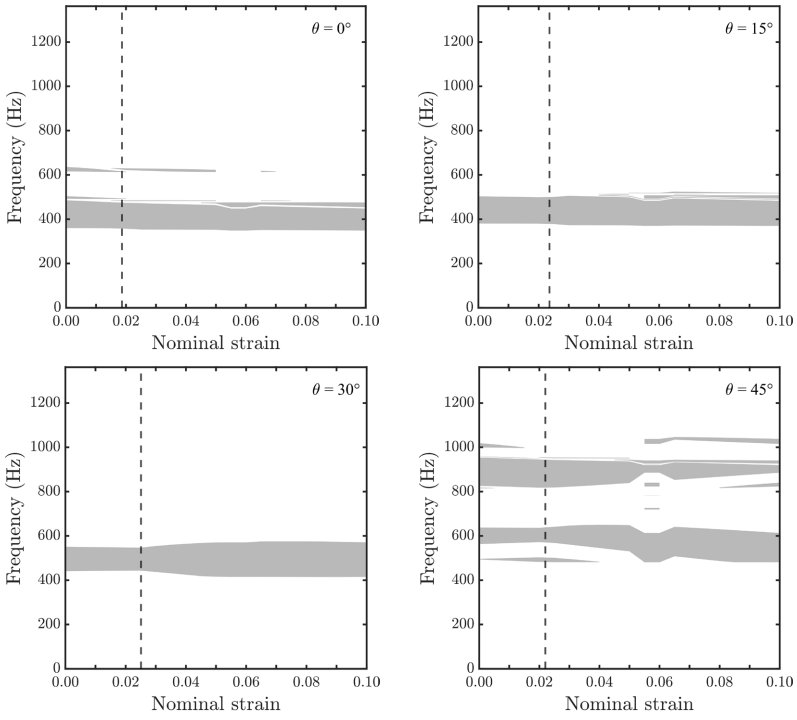

Figure 5. Effects of the nominal strain and of the beam inclination θ on the band gaps (reported as grey regions) of the enlarged unit cell loaded in the z direction. The vertical dotted lines denote as before the values of the nominal strain at the inception of microscopic instability.

- The structure becomes stiffer and the band gaps shift toward higher frequencies. However, when the applied strain also increases, the mean frequency of the lower band gaps decreases, as clearly shown in the solution relevant to $\theta = 45^{\circ}$;
- The effect given by the pattern-induced instability becomes more relevant, *i.e.* the band gap size usually increases after the instability;
- The splitting of the low frequency band gap into smaller band gaps is less frequent. Moreover, for $\theta = 45^{\circ}$ additional band gaps show up at low frequencies.

4. Conclusions

An active truss metamaterial characterized by a three-dimensional periodicity and by a local behavior affected by piezoelectric nanoparticles embedded into a hyperelastic, polymeric matrix has been proposed as an innovative way to exploit geometric and material nonlinearities to actively tune the frequency band gaps.

The composite material has been modelled by extending the typical electric enthalpy density of a linear piezoelectric material to allow for finite deformations. The mechanical energy contribution to the said density has been selected in a form apt to describe compressible Neo-Hookean materials, to take into account the hyperelasticity of the matrix. The tuning of the band gap properties has been then studied by means of instability-induced pattern transformations and by changing the applied compressive strain and a geometric parameter of the primitive unit cell, that is the inclination of some internal beams of the architected unit cell. It has been found that, by increasing the applied strain the band gap gets larger and the range of frequencies of the lower band gap decreases. By increasing instead the aforementioned inclination of the beams, the band gaps tend to shift toward higher frequencies.

What has been presented in this work can be useful to study alternative and more effective ways to improve the tunability of acoustic metamaterial. The results here presented are going to be now extended to allow for poling-induced anisotropy in the response of the architected unit cell, and also assessed via laboratory tests on 3D-printed prototypes of the proposed active metamaterials.

Conflicts of Interest

The authors declare no conflicts of interest regarding the publication of this paper.

References

[1] McFadden, C. (2019) 3 Acoustic Metamaterials You Probably Didn't Know About. https://interestingengineering.com/innovation/3-acoustic-metamaterials-you-probably-didnt-know-about

[2] Bertoldi, K. and Boyce, M.C. (2008) Wave Propagation and Instabilities in Monolithic and Periodically Structured Elastomeric Materials Undergoing Large Defor-

mations. *Phys. Rev. B.*, **78**, Article ID: 184107.
https://doi.org/10.1103/PhysRevB.78.184107

[3] Wang, P., Shim, J. and Bertoldi, K. (2013) Effects of Geometric and Material Nonlinearities on Tunable Band Gaps and Low-Frequency Directionality of Phononic Crystals. *Physical Review B*, **88**, Article ID: 014304.
https://doi.org/10.1103/PhysRevB.88.014304

[4] Bertoldi, K., Boyce, M., Deschanel, S., Prange, S. and Mullin, T. (2008) Mechanics of Deformation-Triggered Pattern Transformations and Superelastic Behavior in Periodic Elastomeric Structures. *Journal of the Mechanics and Physics of Solids*, **56**, 2642-2668. https://doi.org/10.1016/j.jmps.2008.03.006

[5] Akl, W. and Baz, A. (2013) Active Acoustic Metamaterial with Simultaneously Programmable Density and Bulk Modulus. *Journal of Vibration and Acoustics*, **135**, Article ID: 031001. https://doi.org/10.1115/1.4023141

[6] Akl, W. and Baz, A. (2010) Multi-Cell Active Acoustic Metamaterial with Programmable Bulk Modulus. *Journal of Intelligent Material Systems and Structures*, **21**, 541-556. https://doi.org/10.1177/1045389X09359434

[7] Bacigalupo, A., De Bellis, M.L. and Misseroni, D. (2020) Design of Tunable Acoustic Metamaterials with Periodic Piezoelectric Microstructure. *Journal of Intelligent Material Systems and Structures*, **40**, Article ID: 100977.
https://doi.org/10.1016/j.eml.2020.100977

[8] Xia, B., Chen, N., Xie, L., Qin, Y. and Yu, D. (2016) Temperature-Controlled Tunable Acoustic Metamaterial with Active Band Gap and Negative Bulk Modulus. *Applied Acoustics*, **112**, 1-9. https://doi.org/10.1016/j.apacoust.2016.05.005

[9] Chen, X., Xu, X., Ai, S., Chen, H., Pei, Y. and Zhou, X. (2014) Active Acoustic Metamaterials with Tunable Effective Mass Density by Gradient Magnetic Fields. *Applied Physics Letters*, **105**, Article ID: 071913. https://doi.org/10.1063/1.4893921

[10] Bayat, A. (2018) Dynamic Response of Tunable Phononic Crystals and New Homogenization Approaches in Magnetoactive Composites. Ph.D. Thesis, University of Nevada, Reno.

[11] Cui, H., Hensleigh, R., Yao, D., *et al.* (2019) Three-Dimensional Printing of Piezoelectric Materials with Designed Anisotropy and Directional Response. *Nature Materials*, **18**, Article ID: 071913. https://doi.org/10.1038/s41563-018-0268-1

[12] Tiersten, H.F. (1969) Linear Piezoelectric Plate Vibrations. Springer, New York.
https://doi.org/10.1007/978-1-4899-5594-4

[13] Guo, S. (2017) A Coupled Multi-Physics Analysis Model for Integrating Transient ElectroMagnetics and Structural Dynamic Fields with Damage. Ph.D. Thesis, Johns Hopkins University, Baltimore.

[14] COMSOL Multiphysics® v. 6.0. COMSOL AB, Stockholm, Sweden.
https://www.comsol.com/